

**Supporting Information for:**

**CO<sub>2</sub> Methanation Reaction Pathways over Unpromoted and NaNO<sub>3</sub>-Promoted Ru/Al<sub>2</sub>O<sub>3</sub> Catalysts**

Sang Jae Park,<sup>1</sup> Xiang Wang,<sup>2</sup> Madelyn R. Ball,<sup>1</sup> Laura Proano,<sup>1</sup> Zili Wu,<sup>2</sup> Christopher W. Jones<sup>1\*</sup>

<sup>1</sup>School of Chemical & Biomolecular Engineering, Georgia Institute of Technology, 311 Ferst Dr., Atlanta, GA 30332, USA

<sup>2</sup>Chemical Science Division, Oak Ridge National Laboratory, 1 Bethel Valley Road, Oak Ridge, TN 37831, USA

\*Email: [cjones@chbe.gatech.edu](mailto:cjones@chbe.gatech.edu)

I. Supplementary data

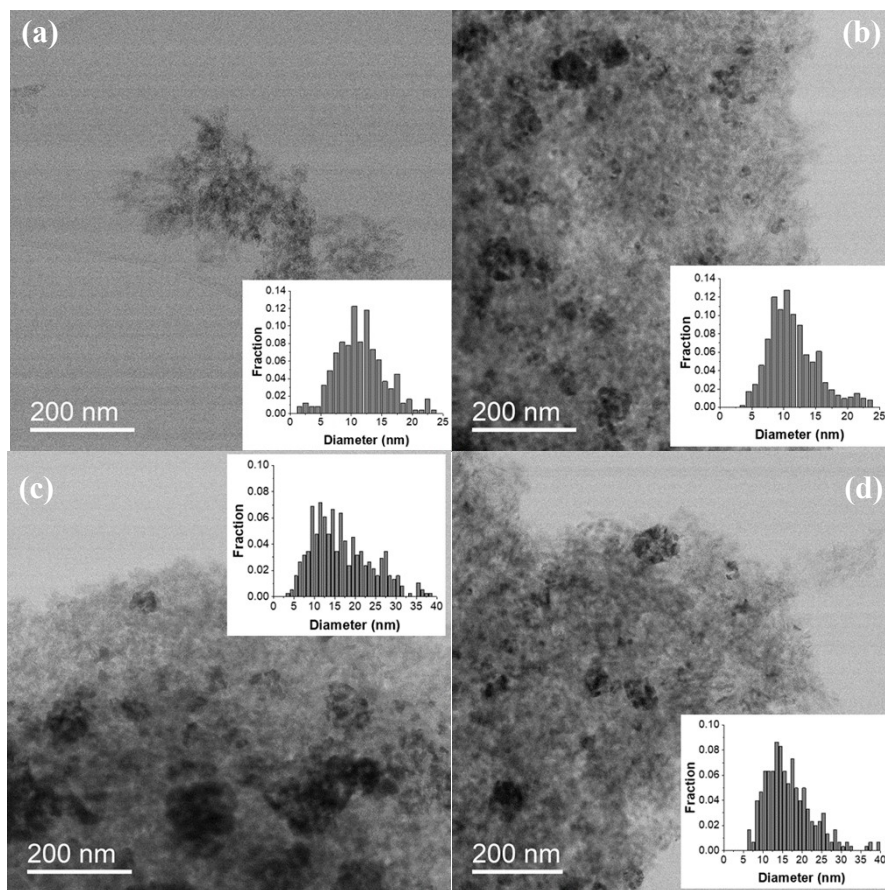


**Figure S1.** TEM images of (a) 1%Ru/Al<sub>2</sub>O<sub>3</sub>, (b) 5%Ru/Al<sub>2</sub>O<sub>3</sub>, (c) NaNO<sub>3</sub>/1%Ru/Al<sub>2</sub>O<sub>3</sub>, and (d) NaNO<sub>3</sub>/5%Ru/Al<sub>2</sub>O<sub>3</sub>.

**Table S1.** Metal dispersion of different catalysts measured by CO chemisorption, assuming stoichiometry of Ru/CO = 1.

	Dispersion - CO chemisorption (%)
1% Ru/Al <sub>2</sub> O <sub>3</sub>	9.3
5% Ru/Al <sub>2</sub> O <sub>3</sub>	8.6
NaNO <sub>3</sub> /1% Ru/Al <sub>2</sub> O <sub>3</sub>	5.3
NaNO <sub>3</sub> /5% Ru/Al <sub>2</sub> O <sub>3</sub>	4.6

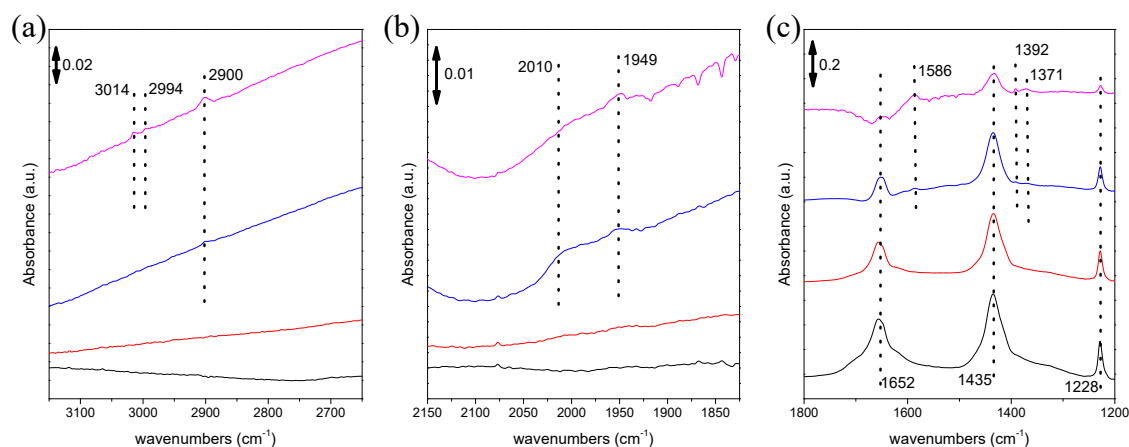


**Figure S2.** DRIFT spectra taken over 1% Ru/Al<sub>2</sub>O<sub>3</sub> under 5%CO<sub>2</sub>/20%H<sub>2</sub>/N<sub>2</sub> flow at 40 mL/min at temperatures of 50 °C (black), 100 °C (red), 200 °C (blue), 300 °C (pink) in the wavelength range of (a) 1200 cm<sup>-1</sup> to 1800 cm<sup>-1</sup>, (b) 1825 cm<sup>-1</sup> to 2150 cm<sup>-1</sup>, and (c) 2650 cm<sup>-1</sup> to 3150 cm<sup>-1</sup>.

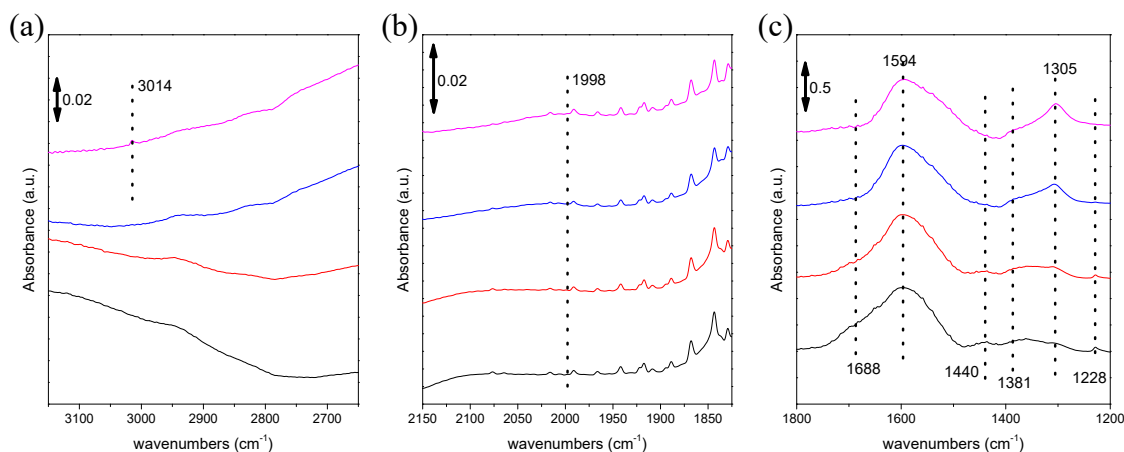


**Figure S3.** DRIFT spectra taken over NaNO<sub>3</sub>/1% Ru/Al<sub>2</sub>O<sub>3</sub> under 5%CO<sub>2</sub>/20%H<sub>2</sub>/N<sub>2</sub> flow at 40 mL/min at temperatures of 50 °C (black), 100 °C (red), 200 °C (blue), 300 °C (pink) at a wavelength range of (a) 1200 cm<sup>-1</sup> to 1800 cm<sup>-1</sup>, (b) 1825 cm<sup>-1</sup> to 2150 cm<sup>-1</sup>, and (c) 2650 cm<sup>-1</sup> to 3150 cm<sup>-1</sup>.

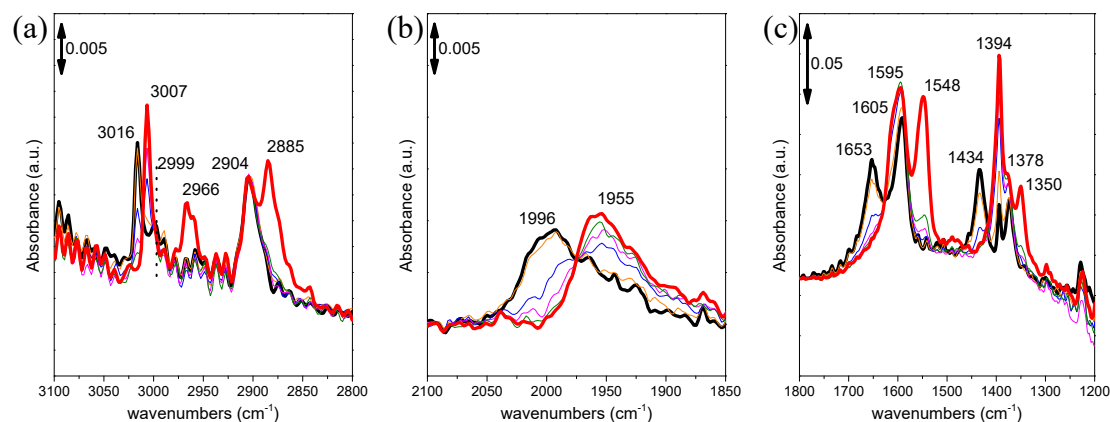


**Figure S4.** *In situ* DRIFT spectra taken over 1% Ru/Al<sub>2</sub>O<sub>3</sub> catalysts at a wavelength range of (a) 1200 cm<sup>-1</sup> to 1800 cm<sup>-1</sup>, (b) 1850 cm<sup>-1</sup> to 2100 cm<sup>-1</sup>, and (c) 2800 cm<sup>-1</sup> to 3100 cm<sup>-1</sup> at a temperature of 260 °C under flow of 5% <sup>12</sup>CO<sub>2</sub>/20% H<sub>2</sub>/N<sub>2</sub> (black, thickened) and after the switch to 5% <sup>13</sup>CO<sub>2</sub>/20% H<sub>2</sub>/N<sub>2</sub> flow. (28 s (orange), 56 s (blue), 85 s (pink), 113 s (green), and 8 min (red, thickened) after the switch).

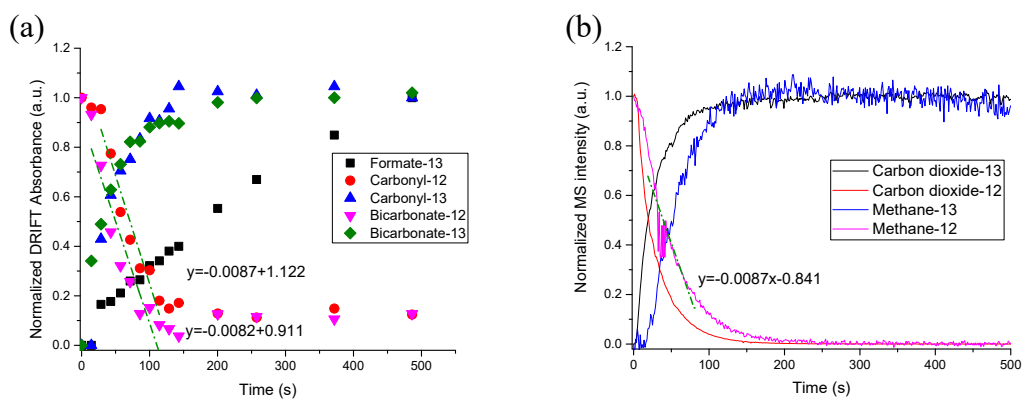


**Figure S5.** (a) Change in normalized DRIFT spectral intensity of observed surface species and (b) change in normalized mass spectroscopy intensity of <sup>12</sup>CO<sub>2</sub>, <sup>13</sup>CO<sub>2</sub>, <sup>12</sup>CH<sub>4</sub>, and <sup>13</sup>CH<sub>4</sub>, after switching from 10% <sup>12</sup>CO<sub>2</sub>/40% H<sub>2</sub>/He flow to 10% <sup>13</sup>CO<sub>2</sub>/40% H<sub>2</sub>/He flow over 1%Ru/Al<sub>2</sub>O<sub>3</sub> catalyst at a temperature of 260 °C. Total flow rate was constant at 40 mL/min.

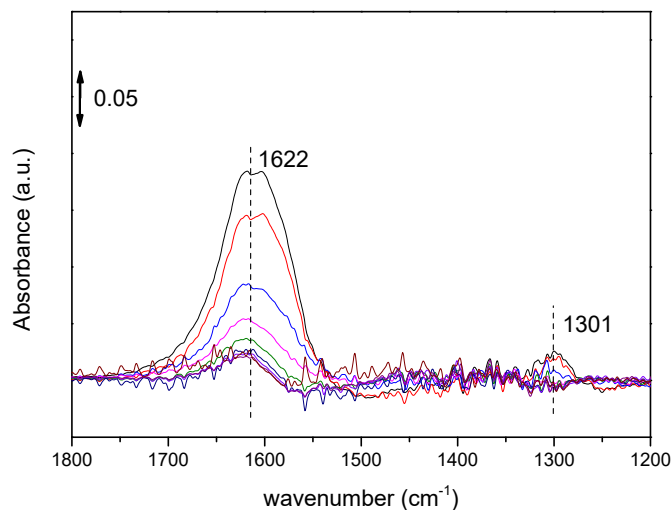


**Figure S6.** *In situ* DRIFT spectra taken over  $\text{NaNO}_3/\text{Al}_2\text{O}_3$  catalysts at wavenumber range of  $1200\text{ cm}^{-1}$  to  $1800\text{ cm}^{-1}$  at temperature of  $260\text{ }^\circ\text{C}$  under flow of  $5\% \text{ }^{12}\text{CO}_2/20\% \text{ H}_2/\text{N}_2$  (black, thickened) and after switch to He flow at constant flow rate of  $40\text{ mL/min}$  (taken every 1 min after the switch).

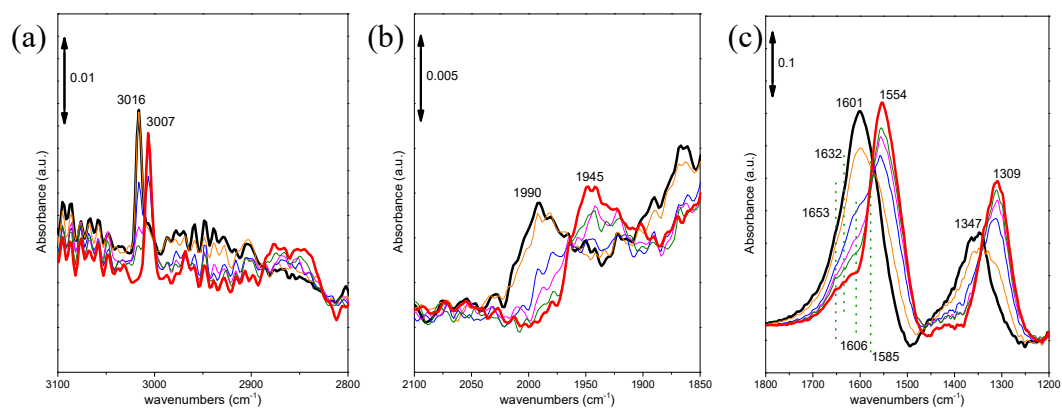


**Figure S7.** *In situ* DRIFT spectra taken over  $\text{NaNO}_3/1\% \text{ Ru}/\text{Al}_2\text{O}_3$  catalysts at a wavelength range of (a)  $1200\text{ cm}^{-1}$  to  $1800\text{ cm}^{-1}$ , (b)  $1850\text{ cm}^{-1}$  to  $2100\text{ cm}^{-1}$ , and (c)  $2800\text{ cm}^{-1}$  to  $3100\text{ cm}^{-1}$  at a temperature of  $260\text{ }^\circ\text{C}$  under a flow of  $5\% \text{ }^{12}\text{CO}_2/20\% \text{ H}_2/\text{N}_2$  (black, thickened) and after switch

to 5%  $^{13}\text{CO}_2/20\%$   $\text{H}_2/\text{N}_2$  flow. (28 s (orange), 56 s (blue), 85 s (pink), 113 s (green), and 8 min (red, thickened) after the switch).

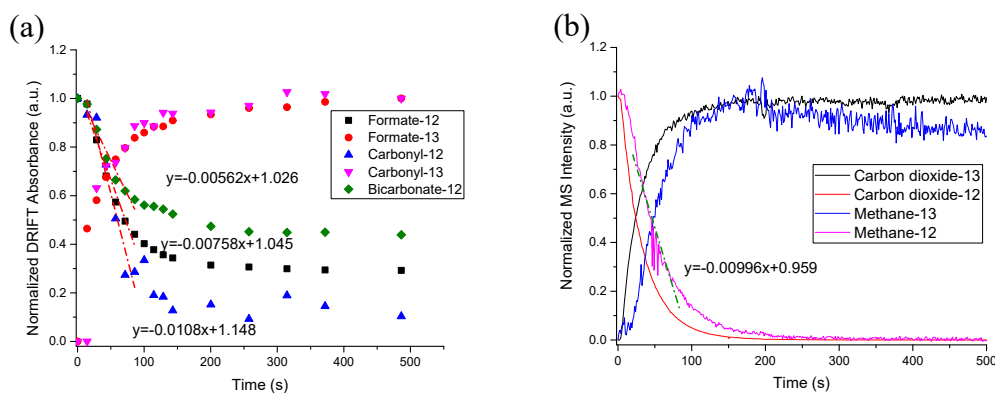


**Figure S8.** (a) Change in normalized DRIFT spectral intensity of observed surface species and (b) change in normalized mass spectroscopy intensity of  $^{12}\text{CO}_2$ ,  $^{13}\text{CO}_2$ ,  $^{12}\text{CH}_4$ , and  $^{13}\text{CH}_4$ , after switching from 10%  $^{12}\text{CO}_2/40\%$   $\text{H}_2/\text{He}$  flow to 10%  $^{13}\text{CO}_2/40\%$   $\text{H}_2/\text{He}$  flow over  $\text{NaNO}_3/1\%\text{Ru}/\text{Al}_2\text{O}_3$  catalysts at a temperature of 260 °C. Total flow rate was constant at 40 mL/min.

## II. Derivation of Rate Equations and Kinetic Fittings over Different Catalysts

**Table S2.** Rate law derivation for the Ru/Al<sub>2</sub>O<sub>3</sub> catalyst for reaction sequence shown in Table 2.

$\frac{d\theta_{OH}}{dt} = r_4 - r_{-4} + r_5 - r_{10} = 0$	Eq.S2-1
$\frac{d\theta_{CO}}{dt} = r_4 - r_{-4} - r_5 = 0$	Eq.S2-2
$2r_5 = r_{10}$	Eq.S2-3
$\theta_{OH} = \frac{2k_5}{k_{10}}\theta_{CO}$	Eq.S2-4
$\theta_H = \theta_* \sqrt{K_1 P_{H_2}}$	Eq.S2-5
$\theta_{CO_2} = \frac{K_3 [CO_3H\#] \theta_*}{[OH\#]} = \frac{K_3 K_2 P_{CO_2} [OH\#] \theta_*}{[OH\#]} = \theta_* K_3 K_2 P_{CO_2}$	Eq.S2-6
$\theta_{CO} = \frac{K_4 \theta_{CO_2} \theta_H}{\theta_{OH}} = \theta_* \frac{\left( k_{10} K_4 K_3 K_2 K_1^2 \right)^{\frac{1}{2}} P_{CO_2}^{\frac{1}{2}} P_{H_2}^{\frac{1}{4}}}{2k_5}$	Eq.S2-7
$\theta_{OH} = \theta_* \frac{\left( 2k_5 K_4 K_3 K_2 K_1^2 \right)^{\frac{1}{2}} P_{CO_2}^{\frac{1}{2}} P_{H_2}^{\frac{1}{4}}}{k_{10}}$	Eq.S2-8
$1 = \theta_* + \theta_H + \theta_{CO_2} + \theta_{CO} + \theta_{OH}$	Eq.S2-9
$\theta_* = \frac{1}{1 + \sqrt{K_1 P_{H_2}} + K_3 K_2 P_{CO_2} + \sqrt{K_4 K_3 K_2 K_1^2 P_{CO_2}^{\frac{1}{2}} P_{H_2}^{\frac{1}{4}} \left( \frac{k_{10}}{2k_5} + \sqrt{\frac{2k_5}{k_{10}}} \right)}}$	Eq.S2-10
$r_5 = k_5 \theta_{CO} \theta_H$	Eq.S2-11
$r_5 = \frac{\left( k_5 k_{10} K_4 K_3 K_2 K_1^2 \right)^{\frac{3}{2}} P_{CO_2}^{\frac{1}{2}} P_{H_2}^{\frac{3}{4}}}{2 \left( 1 + \sqrt{K_1 P_{H_2}} + K_3 K_2 P_{CO_2} + \sqrt{K_4 K_3 K_2 K_1^2 P_{CO_2}^{\frac{1}{2}} P_{H_2}^{\frac{1}{4}} \left( \frac{k_{10}}{2k_5} + \sqrt{\frac{2k_5}{k_{10}}} \right)} \right)^2}$	Eq.S2-12

**Table S3.** Calculated surface coverages of reaction intermediates over 1% Ru/Al<sub>2</sub>O<sub>3</sub> catalysts resulted from regression of experimental data to Eq.(3).

P <sub>CO2</sub> (kPa)	P <sub>H2</sub> (kPa)	$\theta_{\text{H}}$	$\theta_{\text{CO2}}$	$\theta_{\text{CO}}$	$\theta_{\text{OH}}$	$\theta^*$
1.01E+01	4.05E+01	3.39E-01	2.45E-05	2.56E-01	3.91E-03	4.02E-01
2.03E+01	4.05E+01	3.06E-01	4.42E-05	3.26E-01	5.00E-03	3.63E-01
3.04E+01	4.05E+01	2.85E-01	6.17E-05	3.72E-01	5.70E-03	3.38E-01
4.05E+01	4.05E+01	2.69E-01	7.78E-05	4.06E-01	6.22E-03	3.19E-01
1.01E+01	2.03E+01	2.79E-01	2.85E-05	2.50E-01	3.83E-03	4.68E-01
2.03E+01	2.03E+01	2.52E-01	5.16E-05	3.20E-01	4.90E-03	4.23E-01
3.04E+01	2.03E+01	2.35E-01	7.21E-05	3.65E-01	5.59E-03	3.94E-01
4.05E+01	2.03E+01	2.22E-01	9.09E-05	3.99E-01	6.11E-03	3.73E-01
2.03E+01	3.04E+01	2.83E-01	4.72E-05	3.24E-01	4.97E-03	3.88E-01
2.03E+01	5.07E+01	3.24E-01	4.19E-05	3.27E-01	5.01E-03	3.44E-01
4.05E+01	3.04E+01	2.49E-01	8.31E-05	4.04E-01	6.18E-03	3.41E-01
4.05E+01	5.07E+01	2.85E-01	7.37E-05	4.07E-01	6.23E-03	3.02E-01

**Table S4.** Calculated surface coverages of reaction intermediates over 5% Ru/Al<sub>2</sub>O<sub>3</sub> catalysts resulted from regression of experimental data to Eq.(3).

P <sub>CO2</sub> (kPa)	P <sub>H2</sub> (kPa)	$\theta_{\text{H}}$	$\theta_{\text{CO2}}$	$\theta_{\text{CO}}$	$\theta_{\text{OH}}$	$\theta^*$
1.01E+01	4.05E+01	1.78E-01	3.80E-05	2.29E-01	3.77E-03	5.89E-01
2.03E+01	4.05E+01	1.62E-01	6.94E-05	2.95E-01	4.87E-03	5.38E-01
3.04E+01	4.05E+01	1.52E-01	9.75E-05	3.39E-01	5.58E-03	5.04E-01
4.05E+01	4.05E+01	1.44E-01	1.23E-04	3.71E-01	6.12E-03	4.78E-01
1.01E+01	2.03E+01	1.38E-01	4.18E-05	2.11E-01	3.48E-03	6.47E-01
2.03E+01	2.03E+01	1.27E-01	7.67E-05	2.74E-01	4.52E-03	5.94E-01
3.04E+01	2.03E+01	1.19E-01	1.08E-04	3.16E-01	5.21E-03	5.59E-01
4.05E+01	2.03E+01	1.14E-01	1.38E-04	3.48E-01	5.73E-03	5.33E-01
2.03E+01	3.04E+01	1.47E-01	7.25E-05	2.87E-01	4.73E-03	5.61E-01
2.03E+01	5.07E+01	1.75E-01	6.70E-05	3.01E-01	4.97E-03	5.19E-01
4.05E+01	3.04E+01	1.31E-01	1.29E-04	3.62E-01	5.97E-03	5.01E-01
4.05E+01	5.07E+01	1.55E-01	1.19E-04	3.78E-01	6.23E-03	4.60E-01

**Table S5.** Rate law derivation for NaNO<sub>3</sub>/Ru/Al<sub>2</sub>O<sub>3</sub> catalyst for reaction sequence shown in Table 4.

$\frac{d\theta_{CO}}{dt} = r_4 - r_{-4} - r_5 = 0$	Eq.S5-1
$\frac{d\theta_{OH}}{dt} = r_4 - r_{-4} + r_5 - r_{10} = 0$	Eq.S5-2
$\theta_{OH} = \frac{2k_5}{k_{10}}\theta_{CO}$	Eq.S5-3
$\frac{d\theta_C}{dt} = r_5 - r_6 + r_{-6} = 0$	Eq.S5-4
$\frac{d\theta_{CH}}{dt} = r_6 - r_{-6} - r_7 + r_{-7} = 0$	Eq.S5-5
$\frac{d\theta_{CH_2}}{dt} = r_7 - r_{-7} - r_8 + r_{-8} = 0$	Eq.S5-6
$\frac{d\theta_{CH_3}}{dt} = r_8 - r_{-8} - r_9 = 0$	Eq.S5-7
$\theta_{CO} = \frac{k_9}{k_5}\theta_{CH_3}$	Eq.S5-8
$\theta_H = \theta_* \sqrt{K_1 P_{H_2}}$	Eq.S5-9
$\theta_{HCOO} = \frac{K_3[CO_3\#]\theta_H}{[O\#]} = \frac{K_3 K_2 P_{CO_2} [O\#]\theta_H}{[O\#]} = \theta_* K_3 K_2 K_1^{\frac{1}{2}} P_{CO_2}^{\frac{1}{2}} P_{H_2}^{\frac{1}{2}}$	Eq.S5-10
$\theta_{CO} = \frac{K_4 \theta_{HCOO} \theta_*}{\theta_{OH}} = \theta_* \sqrt{\frac{\left(k_{10} K_4 K_3 K_2 K_1^{\frac{1}{2}}\right) P_{CO_2}^{\frac{1}{2}} P_{H_2}^{\frac{1}{4}}}{2k_5}}$	Eq.S5-11
$\theta_{CH_3} = \frac{\theta_*}{k_9} \sqrt{\frac{\left(k_5 k_{10} K_4 K_3 K_2 K_1^{\frac{1}{2}}\right) P_{CO_2}^{\frac{1}{2}} P_{H_2}^{\frac{1}{4}}}{2}}$	Eq.S5-12
$\theta_{OH} = \theta_* \sqrt{\frac{\left(2k_5 K_4 K_3 K_2 K_1^{\frac{1}{2}}\right) P_{CO_2}^{\frac{1}{2}} P_{H_2}^{\frac{1}{4}}}{k_{10}}}$	Eq.S5-13
$\theta_{CH_2} = \frac{\theta_{CH_3} \theta_*}{K_8 \theta_H} = \frac{\theta_*}{k_9 K_8} \sqrt{\frac{\left(k_5 k_{10} K_4 K_3 K_2\right) P_{CO_2}^{\frac{1}{2}} P_{H_2}^{-\frac{1}{4}}}{2K_1^{\frac{1}{2}}}}$	Eq.S5-14

$\theta_{CH} = \frac{\theta_{CH_2} \theta_*}{K_7 \theta_H} = \frac{\theta_*}{k_9 K_7 K_8} \sqrt{\frac{(k_5 k_{10} K_4 K_3 K_2)}{2 K_1^2}} P_{CO_2}^{\frac{1}{2}} P_{H_2}^{-\frac{3}{4}}$	Eq.S5- 15
$\theta_C = \frac{\theta_{CH} \theta_*}{K_6 \theta_H} = \frac{\theta_*}{k_9 K_6 K_7 K_8} \sqrt{\frac{(k_5 k_{10} K_4 K_3 K_2)}{2 K_1^2}} P_{CO_2}^{\frac{1}{2}} P_{H_2}^{-\frac{5}{4}}$	Eq.S5- 16
$1 = \theta_* + \theta_H + \theta_{HCOO} + \theta_{CO} + \theta_{OH} + \theta_C + \theta_{CH} + \theta_{CH_2} + \theta_{CH_3}$	Eq.S5- 17
$\theta_* = \frac{1}{1 + \sqrt{K_1 P_{H_2}} + K_3 K_2 K_1^{\frac{1}{2}} P_{CO_2} P_{H_2}^{\frac{1}{2}} + \sqrt{K_4 K_3 K_2 K_1^{\frac{1}{2}} P_{CO_2}^{\frac{1}{2}} P_{H_2}^{\frac{1}{4}} \left( \sqrt{\frac{k_{10}}{2 k_5}} + \sqrt{\frac{2 k_4}{k_1}} \right)}}$	Eq.S5- 18
$r_9 = k_9 \theta_{CH_3} \theta_H$	Eq.S5- 19
$r_9 = \frac{\sqrt{\frac{(k_5 k_{10} K_4 K_3 K_2)}{2 K_1^2}} P_{CO_2}^{\frac{1}{2}} P_{H_2}^{-\frac{3}{4}}}{\left( 1 + \sqrt{K_1 P_{H_2}} + K_3 K_2 K_1^{\frac{1}{2}} P_{CO_2} P_{H_2}^{\frac{1}{2}} + \sqrt{K_4 K_3 K_2 K_1^{\frac{1}{2}} P_{CO_2}^{\frac{1}{2}} P_{H_2}^{\frac{1}{4}} \left( \sqrt{\frac{k_{10}}{2 k_5}} + \sqrt{\frac{2 k_4}{k_1}} \right)} \right)}$	Eq.S5- 20

**Table S6.** Calculated surface coverages of reaction intermediates over  $\text{NaNO}_3/1\% \text{Ru}/\text{Al}_2\text{O}_3$  catalysts resulted from regression of experimental data to Eq.(4).

P_CO2	P_H2	$\theta_{\text{H}}$	$\theta_{\text{HCOO}}$	$\theta_{\text{CO}}$	$\theta_{\text{C}}$	$\theta_{\text{CH}}$	$\theta_{\text{CH}_2}$	$\theta_{\text{CH}_3}$	$\theta_{\text{OH}}$	$\theta^*$
1.01E+01	4.05E+01	2.97E-01	2.01E-05	7.49E-03	1.94E-01	1.80E-04	1.34E-03	4.93E-01	4.54E-04	0.0063376
2.03E+01	4.05E+01	2.30E-01	3.11E-05	8.22E-03	2.13E-01	1.98E-04	1.47E-03	5.41E-01	4.98E-04	0.0049181
3.04E+01	4.05E+01	1.97E-01	3.99E-05	8.59E-03	2.23E-01	2.07E-04	1.53E-03	5.65E-01	5.21E-04	0.0041968
4.05E+01	4.05E+01	1.75E-01	4.73E-05	8.82E-03	2.29E-01	2.12E-04	1.57E-03	5.81E-01	5.35E-04	0.0037350
1.01E+01	2.03E+01	1.91E-01	1.29E-05	5.71E-03	4.20E-01	2.75E-04	1.44E-03	3.76E-01	3.47E-04	0.0057519
2.03E+01	2.03E+01	1.43E-01	1.93E-05	6.06E-03	4.45E-01	2.92E-04	1.53E-03	3.99E-01	3.68E-04	0.0043153
3.04E+01	2.03E+01	1.20E-01	2.43E-05	6.23E-03	4.58E-01	3.00E-04	1.57E-03	4.10E-01	3.78E-04	0.0036213
4.05E+01	2.03E+01	1.06E-01	2.86E-05	6.33E-03	4.66E-01	3.05E-04	1.60E-03	4.17E-01	3.84E-04	0.0031889
2.03E+01	3.04E+01	1.95E-01	2.63E-05	7.47E-03	2.99E-01	2.40E-04	1.54E-03	4.92E-01	4.53E-04	0.0048051
2.03E+01	5.07E+01	2.56E-01	3.46E-05	8.63E-03	1.60E-01	1.66E-04	1.38E-03	5.68E-01	5.24E-04	0.0048856
4.05E+01	3.04E+01	1.46E-01	3.96E-05	7.93E-03	3.17E-01	2.55E-04	1.64E-03	5.22E-01	4.81E-04	0.0036088
4.05E+01	5.07E+01	1.96E-01	5.30E-05	9.34E-03	1.74E-01	1.80E-04	1.49E-03	6.15E-01	5.67E-04	0.0037402

**Table S7.** Calculated surface coverages of reaction intermediates over  $\text{NaNO}_3/5\% \text{Ru}/\text{Al}_2\text{O}_3$  catalysts resulted from regression of experimental data to Eq.(4).

P_CO2	P_H2	$\theta_{\text{H}}$	$\theta_{\text{HCOO}}$	$\theta_{\text{CO}}$	$\theta_{\text{C}}$	$\theta_{\text{CH}}$	$\theta_{\text{CH}_2}$	$\theta_{\text{CH}_3}$	$\theta_{\text{OH}}$	$\theta^*$
1.01E+01	4.05E+01	1.84E-01	2.09E-05	6.14E-03	2.27E-01	2.09E-04	1.55E-03	5.74E-01	1.00E-03	6.56E-03
2.03E+01	4.05E+01	1.37E-01	3.13E-05	6.51E-03	2.40E-01	2.22E-04	1.64E-03	6.08E-01	1.06E-03	4.92E-03
3.04E+01	4.05E+01	1.15E-01	3.93E-05	6.68E-03	2.47E-01	2.28E-04	1.68E-03	6.24E-01	1.09E-03	4.12E-03
4.05E+01	4.05E+01	1.01E-01	4.61E-05	6.79E-03	2.51E-01	2.31E-04	1.71E-03	6.34E-01	1.11E-03	3.63E-03
1.01E+01	2.03E+01	1.11E-01	1.27E-05	4.43E-03	4.62E-01	3.02E-04	1.57E-03	4.14E-01	7.24E-04	5.63E-03
2.03E+01	2.03E+01	8.15E-02	1.85E-05	4.59E-03	4.79E-01	3.12E-04	1.63E-03	4.28E-01	7.50E-04	4.12E-03
3.04E+01	2.03E+01	6.76E-02	2.31E-05	4.66E-03	4.86E-01	3.17E-04	1.66E-03	4.35E-01	7.62E-04	3.42E-03
4.05E+01	2.03E+01	5.91E-02	2.69E-05	4.70E-03	4.91E-01	3.20E-04	1.67E-03	4.39E-01	7.69E-04	2.99E-03
2.03E+01	3.04E+01	1.14E-01	2.60E-05	5.81E-03	3.30E-01	2.64E-04	1.69E-03	5.42E-01	9.49E-04	4.71E-03
2.03E+01	5.07E+01	1.55E-01	3.52E-05	6.93E-03	1.83E-01	1.89E-04	1.56E-03	6.47E-01	1.13E-03	4.95E-03
4.05E+01	3.04E+01	8.36E-02	3.80E-05	6.02E-03	3.42E-01	2.73E-04	1.75E-03	5.62E-01	9.84E-04	3.45E-03
4.05E+01	5.07E+01	1.15E-01	5.22E-05	7.27E-03	1.92E-01	1.98E-04	1.64E-03	6.79E-01	1.19E-03	3.67E-03

### III. Consideration of Different Reaction Sequences for NaNO<sub>3</sub>/Ru/Al<sub>2</sub>O<sub>3</sub> catalysts

A reaction pathway over NaNO<sub>3</sub>/Ru/Al<sub>2</sub>O<sub>3</sub> catalysts that does not include formate species as a spectator intermediate, as shown in **Table S8**, was considered as well. The reaction pathway differs from the reaction pathway shown in **Table 4** in that a transfer of adsorbed CO<sub>2</sub> on an O# site to the Ru metal site near the metal-support interface to form CO<sub>2</sub>\* is assumed (**Table S8**, step 3), which is followed by a reaction of CO<sub>2</sub>\* with H\* to form linear carbonyl species (**Table S8**, step 4). The derivation of the rate law for this reaction pathway is shown in **Table S9**. Experimental data were fit to the derived rate law, as shown in **Figure S9**, and the simulated surface coverages obtained from kinetic fitting are shown in **Table S10** and **Table S11**. Similar to the reaction sequence shown in **Table 4**, the reaction pathway that does not contain formate as a reaction intermediate also showed a good fit between experimental rates and calculated rates, as shown in **Figure S9**. However, despite the good fit between experimental and calculated rates, the observation of formate peaks at 1600 cm<sup>-1</sup> and 1349 cm<sup>-1</sup> showing a rapid decrease after the switch to <sup>13</sup>CO<sub>2</sub> flow (**Figure 6**) and the similar decomposition rate for <sup>12</sup>CO\* and H<sup>12</sup>COO\* IR peaks observed in the SSITKA experiment (**Figure 7**), suggests that the reaction pathway in **Table 4** is more likely the methanation reaction pathway over NaNO<sub>3</sub>/Ru/Al<sub>2</sub>O<sub>3</sub> catalysts.

**Table S8.** Proposed elementary steps for CO<sub>2</sub> methanation over NaNO<sub>3</sub>/Ru/Al<sub>2</sub>O<sub>3</sub> catalysts assuming formate species are not reaction intermediates.

Step	Reaction
1	H <sub>2</sub> (g) + 2* ↔ 2H*
2	CO <sub>2</sub> (g) + O# ↔ CO <sub>3</sub> #
3	CO <sub>3</sub> # + * ↔ CO <sub>2</sub> * + O#
4	CO <sub>2</sub> * + H* ↔ CO* + OH*
5 (irreversible)	CO* + H* → C* + OH*
6	C* + H* ↔ CH* + *
7	CH* + H* ↔ CH <sub>2</sub> * + *
8	CH <sub>2</sub> * + H* ↔ CH <sub>3</sub> * + *
9 (irreversible)	CH <sub>3</sub> * + H* → CH <sub>4</sub> * + *
10 (irreversible)	OH* + H* → H <sub>2</sub> O* + *
11	CH <sub>4</sub> * ↔ CH <sub>4</sub> (g) + *
12	H <sub>2</sub> O* ↔ H <sub>2</sub> O(g) + *

**Table S9.** Rate law derivation for reaction sequence shown in **Table S8**.

$\frac{d\theta_{CO}}{dt} = r_4 - r_{-4} - r_5 = 0$	Eq.S9-1
$\frac{d\theta_{OH}}{dt} = r_4 - r_{-4} + r_5 - r_{10} = 0$	Eq.S9-2
$\theta_{OH} = \frac{2k_5}{k_{10}}\theta_{CO}$	Eq.S9-3
$\frac{d\theta_C}{dt} = r_5 - r_6 + r_{-6} = 0$	Eq.S9-4
$\frac{d\theta_{CH}}{dt} = r_6 - r_{-6} - r_7 + r_{-7} = 0$	Eq.S9-5
$\frac{d\theta_{CH_2}}{dt} = r_7 - r_{-7} - r_8 + r_{-8} = 0$	Eq.S9-6
$\frac{d\theta_{CH_3}}{dt} = r_8 - r_{-8} - r_9 = 0$	Eq.S9-7
$\theta_{CO} = \frac{k_9}{k_5}\theta_{CH_3}$	Eq.S9-8
$\theta_H = \theta_* \sqrt{K_1 P_{H_2}}$	Eq.S9-9
$\theta_{CO_2} = \frac{K_3 [CO_3\#] \theta_*}{[O\#]} = \frac{K_3 K_2 P_{CO_2} [O\#] \theta_*}{[O\#]} = \theta_* K_3 K_2 P_{CO_2}$	Eq.S9-10

$\theta_{CO} = \frac{K_4 \theta_{CO_2} \theta_H}{\theta_{OH}} = \theta_* \sqrt{\frac{\left(k_{10} K_4 K_3 K_2 K_1^2\right)^{\frac{1}{2}} P_{CO_2}^{\frac{1}{2}} P_{H_2}^{\frac{1}{4}}}{2 k_5}}$	Eq.S9-11
$\theta_{CH_3} = \frac{\theta_*}{k_9} \sqrt{\frac{\left(k_5 k_{10} K_4 K_3 K_2 K_1^2\right)^{\frac{1}{2}} P_{CO_2}^{\frac{1}{2}} P_{H_2}^{\frac{1}{4}}}{2}}$	Eq.S9-12
$\theta_{OH} = \theta_* \sqrt{\frac{\left(2 k_5 K_4 K_3 K_2 K_1^2\right)^{\frac{1}{2}} P_{CO_2}^{\frac{1}{2}} P_{H_2}^{\frac{1}{4}}}{k_{10}}}$	Eq.S9-13
$\theta_{CH_2} = \frac{\theta_{CH_3} \theta_*}{K_8 \theta_H} = \frac{\theta_*}{k_9 K_8} \sqrt{\frac{\left(k_5 k_{10} K_4 K_3 K_2\right)^{\frac{1}{2}} P_{CO_2}^{\frac{1}{2}} P_{H_2}^{-\frac{1}{4}}}{2 K_1^2}}$	Eq.S9-14
$\theta_{CH} = \frac{\theta_{CH_2} \theta_*}{K_7 \theta_H} = \frac{\theta_*}{k_9 K_7 K_8} \sqrt{\frac{\left(k_5 k_{10} K_4 K_3 K_2\right)^{\frac{1}{2}} P_{CO_2}^{\frac{1}{2}} P_{H_2}^{-\frac{3}{4}}}{2 K_1^2}}$	Eq.S9-15
$\theta_C = \frac{\theta_{CH} \theta_*}{K_6 \theta_H} = \frac{\theta_*}{k_9 K_6 K_7 K_8} \sqrt{\frac{\left(k_5 k_{10} K_4 K_3 K_2\right)^{\frac{1}{2}} P_{CO_2}^{\frac{1}{2}} P_{H_2}^{-\frac{5}{4}}}{2 K_1^2}}$	Eq.S9-16
$1 = \theta_* + \theta_H + \theta_{CO_2} + \theta_{CO} + \theta_{OH} + \theta_C + \theta_{CH} + \theta_{CH_2} + \theta_{CH_3}$	Eq.S9-17

$\theta_*$ $= \frac{1}{1 + \sqrt{K_1 P_{H_2}} + K_3 K_2 P_{CO_2} + \sqrt{K_4 K_3 K_2 K_1^{\frac{1}{2}} P_{CO_2}^{\frac{1}{2}} P_{H_2}^{\frac{1}{4}} \left( \sqrt{\frac{k_{10}}{2k_5}} + \sqrt{\frac{2k_5}{k_{10}}} \right)}}$	Eq.S9- 18
$r_9 = k_9 \theta_{CH_3} \theta_H$	Eq.S9- 19
$r_9 = \frac{\sqrt{\frac{(k_5 k_{10} K_4 K_3 K_1^{\frac{1}{2}} P_{CO_2}^{\frac{1}{2}} P_{H_2}^{\frac{1}{4}})}{2}}}{1 + \sqrt{K_1 P_{H_2}} + K_3 K_2 P_{CO_2} + \sqrt{K_4 K_3 K_2 K_1^{\frac{1}{2}} P_{CO_2}^{\frac{1}{2}} P_{H_2}^{\frac{1}{4}} \left( \sqrt{\frac{k_{10}}{2k_5}} + \sqrt{\frac{2k_5}{k_{10}}} \right)}}$	Eq.S9- 20

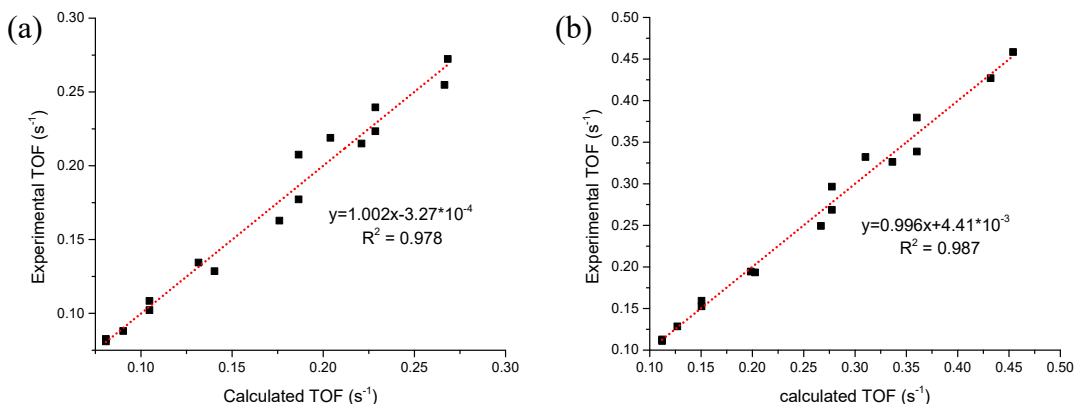


**Figure S9.** Calculated TOFs vs experimental TOFs for (a) NaNO<sub>3</sub>/1% Ru/Al<sub>2</sub>O<sub>3</sub> and (b) NaNO<sub>3</sub>/5% Ru/Al<sub>2</sub>O<sub>3</sub> according to rate law derived in Eq.S9-20.

**Table S10.** Calculated kinetic constants for NaNO<sub>3</sub>/1% Ru/Al<sub>2</sub>O<sub>3</sub> and NaNO<sub>3</sub>/5% Ru/Al<sub>2</sub>O<sub>3</sub> catalysts resulted from regression of experimental data to Eq.S9-20.

Kinetic constants	NaNO <sub>3</sub> /1% Ru/Al <sub>2</sub> O <sub>3</sub>	NaNO <sub>3</sub> /5% Ru/Al <sub>2</sub> O <sub>3</sub>
K <sub>1</sub> (kPa <sup>-1</sup> )	791 ± 48.8	111 ± 18.6
K <sub>2</sub> K <sub>3</sub> (kPa <sup>-1</sup> )	6.24 x 10 <sup>-6</sup> ± 5.67 x 10 <sup>-7</sup>	1.49 x 10 <sup>-5</sup> ± 3.08 x 10 <sup>-6</sup>
K <sub>4</sub>	6.24 ± 0.56	1.48 ± 0.329
k <sub>5</sub> (s <sup>-1</sup> )	2504 ± 225	6293 ± 1776
K <sub>6</sub>	1.21 x 10 <sup>-5</sup> ± 4.49 x 10 <sup>-7</sup>	9.08 x 10 <sup>-5</sup> ± 1.99 x 10 <sup>-5</sup>
K <sub>7</sub>	6.06 x 10 <sup>-3</sup> ± 2.24 x 10 <sup>-4</sup>	0.0135 ± 1.97 x 10 <sup>-3</sup>
K <sub>8</sub>	6.03 ± 0.226	7.24 ± 4.95
k <sub>9</sub> (s <sup>-1</sup> )	1.78 ± 0.0901	4.14 ± 0.311
k <sub>10</sub> (s <sup>-1</sup> )	3135 ± 283	1.56 x 10 <sup>4</sup> ± 3310

**Table S11.** Calculated surface coverages of reaction intermediates over  $\text{NaNO}_3/1\% \text{Ru}/\text{Al}_2\text{O}_3$  catalysts resulted from regression of experimental data to Eq.S9-20.

P_CO2	P_H2	$\theta_{\text{H}}$	$\theta_{\text{CO}_2}$	$\theta_{\text{CO}}$	$\theta_{\text{C}}$	$\theta_{\text{CH}}$	$\theta_{\text{CH}_2}$	$\theta_{\text{CH}_3}$	$\theta_{\text{OH}}$	$\theta^*$
1.01E+01	4.05E+01	3.02E-01	1.07E-07	3.55E-04	1.95E-01	4.24E-04	4.60E-04	4.99E-01	5.67E-04	1.69E-03
2.03E+01	4.05E+01	2.34E-01	1.66E-07	3.89E-04	2.14E-01	4.65E-04	5.05E-04	5.48E-01	6.22E-04	1.31E-03
3.04E+01	4.05E+01	2.00E-01	2.12E-07	4.07E-04	2.24E-01	4.86E-04	5.28E-04	5.73E-01	6.50E-04	1.12E-03
4.05E+01	4.05E+01	1.78E-01	2.52E-07	4.18E-04	2.30E-01	5.00E-04	5.42E-04	5.89E-01	6.68E-04	9.94E-04
1.01E+01	2.03E+01	1.94E-01	9.69E-08	2.71E-04	4.21E-01	6.47E-04	4.97E-04	3.81E-01	4.33E-04	1.53E-03
2.03E+01	2.03E+01	1.45E-01	1.45E-07	2.87E-04	4.47E-01	6.86E-04	5.27E-04	4.05E-01	4.59E-04	1.15E-03
3.04E+01	2.03E+01	1.22E-01	1.83E-07	2.95E-04	4.59E-01	7.05E-04	5.41E-04	4.16E-01	4.72E-04	9.63E-04
4.05E+01	2.03E+01	1.07E-01	2.15E-07	3.00E-04	4.67E-01	7.17E-04	5.50E-04	4.23E-01	4.80E-04	8.48E-04
2.03E+01	3.04E+01	1.98E-01	1.62E-07	3.54E-04	3.00E-01	5.64E-04	5.30E-04	4.99E-01	5.66E-04	1.28E-03
2.03E+01	5.07E+01	2.60E-01	1.64E-07	4.09E-04	1.61E-01	3.91E-04	4.74E-04	5.76E-01	6.53E-04	1.30E-03
4.05E+01	3.04E+01	1.49E-01	2.43E-07	3.76E-04	3.18E-01	5.99E-04	5.63E-04	5.30E-01	6.01E-04	9.60E-04
4.05E+01	5.07E+01	1.99E-01	2.52E-07	4.43E-04	1.74E-01	4.23E-04	5.13E-04	6.23E-01	7.08E-04	9.95E-04

**Table S12.** Calculated surface coverages of reaction intermediates over  $\text{NaNO}_3/5\% \text{Ru}/\text{Al}_2\text{O}_3$  catalysts resulted from regression of experimental data to Eq.S9-20.

P_CO2	P_H2	$\theta_{\text{H}}$	$\theta_{\text{CO}_2}$	$\theta_{\text{CO}}$	$\theta_{\text{C}}$	$\theta_{\text{CH}}$	$\theta_{\text{CH}_2}$	$\theta_{\text{CH}_3}$	$\theta_{\text{OH}}$	$\theta^*$
1.01E+01	4.05E+01	1.90E-01	4.27E-07	3.86E-04	2.19E-01	1.33E-03	1.21E-03	5.86E-01	3.12E-04	2.83E-03
2.03E+01	4.05E+01	1.42E-01	6.40E-07	4.09E-04	2.32E-01	1.41E-03	1.28E-03	6.21E-01	3.31E-04	2.12E-03
3.04E+01	4.05E+01	1.19E-01	8.05E-07	4.20E-04	2.38E-01	1.45E-03	1.31E-03	6.37E-01	3.40E-04	1.78E-03
4.05E+01	4.05E+01	1.05E-01	9.45E-07	4.27E-04	2.42E-01	1.47E-03	1.33E-03	6.48E-01	3.45E-04	1.57E-03
1.01E+01	2.03E+01	1.16E-01	3.70E-07	2.81E-04	4.51E-01	1.94E-03	1.24E-03	4.27E-01	2.27E-04	2.46E-03
2.03E+01	2.03E+01	8.53E-02	5.42E-07	2.92E-04	4.67E-01	2.01E-03	1.29E-03	4.42E-01	2.36E-04	1.80E-03
3.04E+01	2.03E+01	7.08E-02	6.75E-07	2.96E-04	4.74E-01	2.04E-03	1.31E-03	4.49E-01	2.39E-04	1.49E-03
4.05E+01	2.03E+01	6.19E-02	7.87E-07	2.99E-04	4.79E-01	2.06E-03	1.32E-03	4.54E-01	2.42E-04	1.31E-03
2.03E+01	3.04E+01	1.19E-01	6.16E-07	3.67E-04	3.20E-01	1.68E-03	1.32E-03	5.56E-01	2.96E-04	2.04E-03
2.03E+01	5.07E+01	1.60E-01	6.43E-07	4.35E-04	1.76E-01	1.20E-03	1.21E-03	6.59E-01	3.51E-04	2.13E-03
4.05E+01	3.04E+01	8.70E-02	9.04E-07	3.80E-04	3.31E-01	1.75E-03	1.37E-03	5.76E-01	3.07E-04	1.50E-03
4.05E+01	5.07E+01	1.19E-01	9.54E-07	4.56E-04	1.85E-01	1.26E-03	1.27E-03	6.92E-01	3.68E-04	1.58E-03

Combining observations made in our previous work, in which the carbonyl IR peaks over  $\text{Ru}/\text{Al}_2\text{O}_3$  and  $\text{NaNO}_3/\text{Ru}/\text{Al}_2\text{O}_3$  observed during methanation reaction conditions, and previous reports that hydrogen carbonyl species ( $\text{H}^*\text{CO}$  or  $(2\text{H})^*\text{CO}$ ) could be formed as reaction intermediates during  $\text{CO}_2$  methanation, a reaction pathway that includes hydrogen carbonyl species was also considered as reaction pathway over  $\text{NaNO}_3/\text{Ru}/\text{Al}_2\text{O}_3$  catalysts.<sup>1,2</sup> This reaction sequence is shown in **Table S12**, and the derivation of the rate law for the reaction sequence is shown in **Table S13**. As observed in **Figure S10**, the hydrogen carbonyl pathway also showed a good fit of the experimental TOF values to the derived rate law for both  $\text{NaNO}_3/1\%\text{Ru}/\text{Al}_2\text{O}_3$  and  $\text{NaNO}_3/5\%\text{Ru}/\text{Al}_2\text{O}_3$  catalysts, showing slopes of nearly 1 and  $R^2$  values of 0.971 and 0.984.

However, this pathway is likely not the main reaction pathway for CO<sub>2</sub> methanation over NaNO<sub>3</sub>/Ru/Al<sub>2</sub>O<sub>3</sub> catalysts, because the surface coverage of hydrogen is quite high, which is not consistent with the high H<sub>2</sub> reaction order observed for the NaNO<sub>3</sub>/Ru/Al<sub>2</sub>O<sub>3</sub> catalysts, implying low surface coverage of hydrogen. For H\*CO and 2H\*CO species, hydrogen atoms are directly attached to Ru active sites, and the surface coverage of H\*, H\*CO, and (2H)\*CO combined, ranges from approximately 0.30 to 0.49 for NaNO<sub>3</sub>/1%Ru/Al<sub>2</sub>O<sub>3</sub> and 0.21 to 0.37 for NaNO<sub>3</sub>/5%Ru/Al<sub>2</sub>O<sub>3</sub> under the given experimental conditions, as shown in **Table S14** and **Table S15**. These values are higher than the hydrogen surface coverage observed over unpromoted Ru/Al<sub>2</sub>O<sub>3</sub> catalysts, as 1%Ru/Al<sub>2</sub>O<sub>3</sub> showed H\* surface coverages between 0.22 and 0.34, and 5% Ru/Al<sub>2</sub>O<sub>3</sub> showed H\* surface coverages between 0.11 and 0.18 under the given experimental conditions, as shown in **Table S3** and **Table S4**. This higher surface coverage of hydrogen on the metal surface does not align with the implications of increased H<sub>2</sub> reaction orders, making the hydrogen carbonyl reaction pathway less likely. With the further information gathered from the kinetic modeling results, it is concluded that the difference in the IR spectra between 1%Ru/Al<sub>2</sub>O<sub>3</sub> and NaNO<sub>3</sub>/1%Ru/Al<sub>2</sub>O<sub>3</sub> in our previous work is most likely not due to presence of hydrogen carbonyl species. Rather it is possible that higher coverage of other carbonyl species, such as dicarbonyl or tricarbonyl species, caused slight shift to higher wavenumbers for the case of the 1% Ru/Al<sub>2</sub>O<sub>3</sub>, as the *in situ* FTIR experiment was performed under different reaction conditions with higher CO<sub>2</sub> partial pressure than the conditions performed in this work.

After consideration of several different possible reaction pathways, we conclude that the reaction pathway shown in **Table 4**, which includes bidentate carbonate, formate, and linear carbonyl species as reaction intermediates and assumes an additional irreversible step of

hydrogenation of  $\text{CH}_3^*$  in the formation of methane, is the most representative reaction pathway for  $\text{CO}_2$  methanation over  $\text{NaNO}_3/\text{Ru}/\text{Al}_2\text{O}_3$  catalysts under the conditions employed.

**Table S13.** Proposed elementary steps for  $\text{CO}_2$  methanation over  $\text{NaNO}_3/\text{Ru}/\text{Al}_2\text{O}_3$  catalysts, using hydrogen carbonyl species as reaction intermediate.

Step	Reaction
1	$\text{H}_2(\text{g}) + 2^* \leftrightarrow 2\text{H}^*$
2	$\text{CO}_2(\text{g}) + \text{O}\# \leftrightarrow \text{CO}_3\#$
3	$\text{CO}_3\# + \text{H}^* \leftrightarrow \text{HCOO}^* + \text{O}\#$
4	$\text{HCOO}^* + ^* \leftrightarrow \text{CO}^* + \text{OH}^*$
5	$\text{CO}^* + \text{H}^* \leftrightarrow \text{H}^*\text{CO} + ^*$
6	$\text{H}^*\text{CO} + \text{H}^* \leftrightarrow (2\text{H})^*\text{CO} + ^*$
7 (RDS)	$\text{H}_2^*\text{CO} + \text{H}^* \rightarrow \text{CH}_2^* + \text{OH}^*$
8	$\text{CH}_2^{*+*} + \text{H}^* \leftrightarrow \text{CH}_3^* + ^*$
9	$\text{CH}_3^* + \text{H}^* \leftrightarrow \text{CH}_4^* + ^*$
10	$\text{CH}_4^* \leftrightarrow \text{CH}_4(\text{g}) + ^*$
11 (irreversible)	$\text{OH}^* + \text{H}^* \rightarrow \text{H}_2\text{O}^* + ^*$
12	$\text{H}_2\text{O}^* \leftrightarrow \text{H}_2\text{O}(\text{g}) + ^*$

**Table S14.** Rate law derivation for reaction sequence shown in **Table S13**.

$\frac{d\theta_{\text{CO}}}{dt} = r_4 - r_{-4} - r_5 + r_{-5} = 0$	Eq. S14-1
$\frac{d\theta_{\text{H}^*\text{CO}}}{dt} = r_5 - r_{-5} - r_6 + r_{-6} = 0$	Eq. S14-2
$\frac{d\theta_{\text{H}_2^*\text{CO}}}{dt} = r_6 - r_{-6} - r_7 = 0$	Eq. S14-3
$\frac{d\theta_{\text{OH}}}{dt} = r_4 - r_{-4} + r_7 - r_{11} = 0$	Eq. S14-4
$\theta_{\text{OH}} = \frac{2k_7}{k_{11}}\theta_{\text{H}_2^*\text{CO}}$	Eq. S14-5
$\theta_{\text{H}} = \theta_* \sqrt{K_1 P_{\text{H}_2}}$	Eq. S14-6

$\theta_{HCOO} = \frac{K_3[CO_3\#]\theta_H}{[O\#]} = \frac{K_3K_2P_{CO_2}[O\#]\theta_H}{[O\#]} = \theta_* K_3K_2K_1^{\frac{1}{2}}P_{CO_2}^{\frac{1}{2}}P_{H_2}^{\frac{1}{2}}$	Eq. S14-7
$\theta_{CO} = \frac{K_4\theta_{HCOO}\theta_*}{\theta_{OH}} = \theta_* \sqrt{\frac{(k_{11}K_4K_3K_2) \frac{1}{2} P_{CO_2}^{\frac{1}{2}} P_{H_2}^{-\frac{1}{4}}}{2k_7K_6K_5K_1^{\frac{1}{2}}}}$	Eq. S14-8
$\theta_{H^*CO} = \frac{K_5\theta_{CO}\theta_H}{\theta_*} = \theta_* \sqrt{\frac{\left(k_{11}K_5K_4K_3K_2K_1^{\frac{1}{2}}\right) P_{CO_2}^{\frac{1}{2}} P_{H_2}^{\frac{1}{4}}}{2k_7K_6}}$	Eq. S14-9
$\theta_{H_2^*CO} = \frac{K_6\theta_{H^*CO}\theta_H}{\theta_*} = \theta_* \sqrt{\frac{\left(k_{11}K_6K_5K_4K_3K_2K_1^{\frac{1}{2}}\right)^3 P_{CO_2}^{\frac{1}{2}} P_{H_2}^{\frac{3}{4}}}{2k_7}}$	Eq. S14-10
$\theta_{OH} = \theta_* \sqrt{\frac{\left(2k_7K_6K_5K_4K_3K_2K_1^{\frac{1}{2}}\right)^3 P_{CO_2}^{\frac{1}{2}} P_{H_2}^{\frac{3}{4}}}{k_{11}}}$	Eq. S14-11
$1 = \theta_* + \theta_H + \theta_{HCOO} + \theta_{CO} + \theta_{H^*CO} + \theta_{H_2^*CO} + \theta_{OH}$	Eq. S14-12
$\theta_* = \frac{1}{1 + \sqrt{K_1P_{H_2}}(1 + K_3K_2P_{CO_2}) + \sqrt{K_4K_3K_2}P_{CO_2}^{\frac{1}{2}} \left( \frac{k_{11}}{2k_7K_6K_5K_1^{\frac{1}{2}}} \right)^{\frac{1}{2}}}$	Eq. S14-13
$r_7 = k_7\theta_{H_2^*CO}\theta_H$	Eq. S14-14
$r = \frac{\sqrt{\frac{k_7k_{11}K_6K_5K_4K_3}{2}}}{\left(1 + \sqrt{K_1P_{H_2}}(1 + K_3K_2P_{CO_2}) + \sqrt{K_4K_3K_2}P_{CO_2}^{\frac{1}{2}} \left( \frac{k_{11}}{2k_7K_6K_5K_1^{\frac{1}{2}}} \right)^{\frac{1}{2}}\right)}$	Eq. S14-15

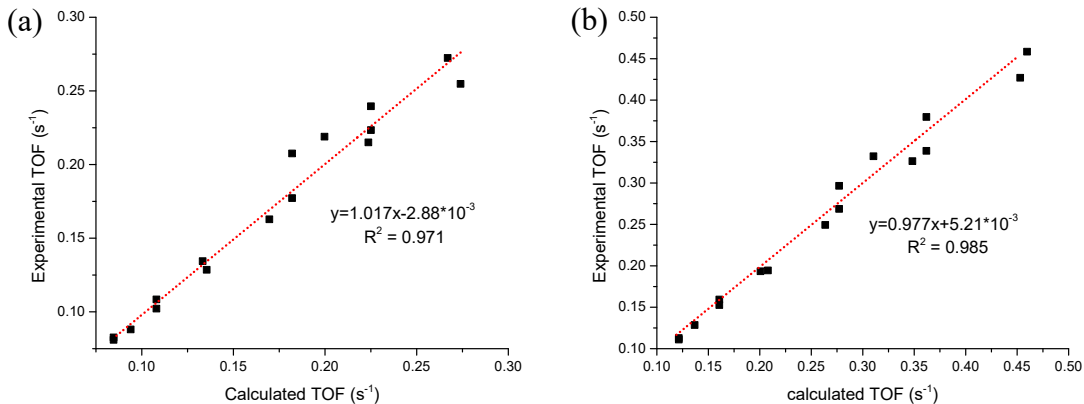


**Figure S10.** Calculated TOFs vs experimental TOFs for (a)  $\text{NaNO}_3/1\% \text{Ru}/\text{Al}_2\text{O}_3$  and (b)  $\text{NaNO}_3/5\% \text{Ru}/\text{Al}_2\text{O}_3$  using rate law derived Eq.S14-15.

**Table S15.** Calculated kinetic constants for  $\text{NaNO}_3/1\% \text{Ru}/\text{Al}_2\text{O}_3$  and  $\text{NaNO}_3/5\% \text{Ru}/\text{Al}_2\text{O}_3$  catalysts resulted from regression of experimental data to Eq.S14-15.

Kinetic constants	$\text{NaNO}_3/1\% \text{Ru}/\text{Al}_2\text{O}_3$	$\text{NaNO}_3/5\% \text{Ru}/\text{Al}_2\text{O}_3$
$K_1$ ( $\text{kPa}^{-1}$ )	$12.1 \pm 0.949$	$0.0991 \pm 0.0293$
$K_2 K_3$ ( $\text{kPa}^{-1}$ )	$9.02 \times 10^{-6} \pm 1.55 \times 10^{-6}$	$8.18 \times 10^{-6} \pm 1.27 \times 10^{-6}$
$K_4$	$2221 \pm 350$	$823 \pm 129$
$K_5$	$1.96 \times 10^{-5} \pm 1.54 \times 10^{-6}$	$0.0498 \pm 7.49 \times 10^{-4}$
$K_6$	$49.0 \pm 3.86$	$2.15 \pm 0.591$
$k_7$ ( $\text{s}^{-1}$ )	$4.26 \pm 0.431$	$16.7 \pm 1.69$
$k_{11}$ ( $\text{s}^{-1}$ )	$1351 \pm 541$	$8549 \pm 1475$

**Table S16.** Calculated surface coverages of reaction intermediates over  $\text{NaNO}_3/1\% \text{ Ru}/\text{Al}_2\text{O}_3$  catalysts resulted from regression of experimental data to Eq.S14-15.

P_CO2	P_H2	$\theta_{\text{H}}$	$\theta_{\text{HCOO}}$	$\theta_{\text{CO}}$	$\theta_{\text{H}^*\text{CO}}$	$\theta_{\text{H}_2^*\text{CO}}$	$\theta_{\text{OH}}$	$\theta^*$
10.1325	40.53	2.75E-01	2.52E-05	4.83E-01	2.10E-04	2.28E-01	1.44E-03	1.24E-02
20.265	40.53	2.12E-01	3.88E-05	5.27E-01	2.29E-04	2.49E-01	1.57E-03	9.58E-03
30.3975	40.53	1.81E-01	4.96E-05	5.50E-01	2.39E-04	2.59E-01	1.63E-03	8.16E-03
40.53	40.53	1.61E-01	5.88E-05	5.64E-01	2.45E-04	2.66E-01	1.68E-03	7.25E-03
10.1325	20.265	2.12E-01	1.94E-05	6.26E-01	1.92E-04	1.48E-01	9.30E-04	1.35E-02
20.265	20.265	1.61E-01	2.93E-05	6.70E-01	2.06E-04	1.58E-01	9.96E-04	1.02E-02
30.3975	20.265	1.35E-01	3.71E-05	6.92E-01	2.12E-04	1.63E-01	1.03E-03	8.63E-03
40.53	20.265	1.19E-01	4.37E-05	7.05E-01	2.17E-04	1.66E-01	1.05E-03	7.62E-03
20.265	30.3975	1.91E-01	3.50E-05	5.89E-01	2.22E-04	2.08E-01	1.31E-03	9.96E-03
20.265	50.6625	2.28E-01	4.17E-05	4.79E-01	2.32E-04	2.82E-01	1.78E-03	9.20E-03
40.53	30.3975	1.44E-01	5.25E-05	6.26E-01	2.35E-04	2.21E-01	1.40E-03	7.48E-03
40.53	50.6625	1.73E-01	6.33E-05	5.14E-01	2.50E-04	3.03E-01	1.91E-03	6.99E-03

**Table S17.** Calculated surface coverages of reaction intermediates over  $\text{NaNO}_3/5\% \text{ Ru}/\text{Al}_2\text{O}_3$  catalysts resulted from regression of experimental data to Eq.S14-15.

P_CO2	P_H2	$\theta_{\text{H}}$	$\theta_{\text{HCOO}}$	$\theta_{\text{CO}}$	$\theta_{\text{H}^*\text{CO}}$	$\theta_{\text{H}_2^*\text{CO}}$	$\theta_{\text{OH}}$	$\theta^*$
10.1325	40.53	1.19E-01	9.88E-06	5.36E-01	5.35E-02	2.31E-01	9.02E-04	5.95E-02
20.265	40.53	8.89E-02	1.47E-05	5.66E-01	5.64E-02	2.43E-01	9.52E-04	4.44E-02
30.3975	40.53	7.44E-02	1.85E-05	5.80E-01	5.78E-02	2.50E-01	9.76E-04	3.71E-02
40.53	40.53	6.54E-02	2.17E-05	5.89E-01	5.87E-02	2.53E-01	9.91E-04	3.26E-02
10.1325	20.265	8.74E-02	7.25E-06	6.61E-01	4.66E-02	1.42E-01	5.56E-04	6.17E-02
20.265	20.265	6.46E-02	1.07E-05	6.92E-01	4.88E-02	1.49E-01	5.82E-04	4.56E-02
30.3975	20.265	5.39E-02	1.34E-05	7.06E-01	4.98E-02	1.52E-01	5.94E-04	3.80E-02
40.53	20.265	4.72E-02	1.57E-05	7.15E-01	5.04E-02	1.54E-01	6.01E-04	3.33E-02
20.265	30.3975	7.87E-02	1.30E-05	6.21E-01	5.36E-02	2.00E-01	7.84E-04	4.53E-02
20.265	50.6625	9.68E-02	1.60E-05	5.21E-01	5.81E-02	2.80E-01	1.10E-03	4.32E-02
40.53	30.3975	5.77E-02	1.91E-05	6.45E-01	5.57E-02	2.08E-01	8.13E-04	3.33E-02
40.53	50.6625	7.13E-02	2.37E-05	5.43E-01	6.06E-02	2.92E-01	1.14E-03	3.18E-02

#### IV. Mass transfer limitation analysis

Calculations were performed to confirm mass transfer limitations are negligible. It should be noted that thermophysical properties of different gases were obtained from NIST WebBook, Thermophysical Properties of Fluid Systems, unless noted otherwise.<sup>3</sup> Internal mass transfer limitations were assessed by using the Weisz-Prater Criterion, as shown in Eq. (S16).<sup>4,5</sup> This specific sample calculation shows 10% CO<sub>2</sub> concentration over 5% NaNO<sub>3</sub>/5% Ru/Al<sub>2</sub>O<sub>3</sub> at 280 °C, which gave the highest value for the Weisz-Prater parameter.

$$\varphi = - \frac{r_{obs} * \rho_p * R_p}{D_e * C_{AS}} \quad \text{Eq. (S16)}$$

The concentration of CO<sub>2</sub> at the external particle surface,  $C_{AS}$ , was 0.00409 mmol/mL. The radius of the catalyst particle,  $R_p$ , was 0.0138 cm. For calculation of the effective diffusivity,  $D_e$ , Knudsen diffusivity was calculated based on Eq. (S17).

$$D_e = \frac{d}{3} \sqrt{\frac{8 * R * T}{\pi * M_A}} \quad \text{Eq. (S17)}$$

Pore diameter,  $d$ , was  $2.1 \times 10^{-8}$  m, which was obtained by N<sub>2</sub> physisorption measurement. Molecular mass,  $M_A$ , of 44.01 g/mol, temperature,  $T$ , of 553 K (280 °C), and gas constant,  $R$ , of 8.314 J/mol-K were used to obtain an effective diffusivity of 0.0361 cm<sup>2</sup>/s. The rate observed,  $r_{obs}$  was 0.020 mmol CO<sub>2</sub>/s-g<sub>cat</sub>. The bulk density of the catalyst,  $\rho_p$ , was 4 g/mL. From Eq. (S16), the WPN parameter was calculated to be 0.102, which is much smaller than 1, indicating that the internal mass transfer limitations were negligible.

External mass transfer limitations were assessed using the Mears criterion, as shown in Eq. (S18).  $M_{ext}$  lower than 0.15 indicates that the external mass transfer limitations can be neglected.<sup>6</sup> It should be noted that for calculation of  $M_{ext}$ ,  $H_2$  parameters were used, because the  $CO_2$  reaction order was found to be negative for the 5%  $NaNO_3/5\%Ru/Al_2O_3$  catalyst. To obtain the mass transfer coefficient, the Reynolds number was calculated using Eq. (S19).

$$M_{ext} = -\frac{r_{obs} * \rho_p * L * n}{k_c * C_{AS}} \quad \text{Eq. (S18)}$$

$$Re = \frac{2 * U * L}{\nu} \quad \text{Eq. (S19)}$$

The superficial velocity,  $U$ , was 0.0195 m/s. and the particle size of the pellet,  $L$ , was 0.0138 cm. Kinematic viscosity of  $N_2$  ( $4.60 \times 10^{-5}$  m<sup>2</sup>/s) was used for conservative  $Re$  calculation, since the feed gas mixture was mostly composed of  $N_2$  and  $H_2$ , but  $N_2$  has lower kinematic viscosity leading to higher  $Re$ . Plugging in such values to Eq. S19,  $Re$  of 0.12 can be calculated, which was much less than 1. This means the mass transfer coefficient could be estimated by Eq. (S20).

$$Sh = \frac{k_c * 2 * L}{D_e} = 2 \quad \text{Eq. (S20)}$$

The bulk diffusivity of  $H_2$ - $N_2$  was used as  $D_e$  in Eq. (S20), which was estimated to be 2.26 cm<sup>2</sup>/s at 280 °C.<sup>7</sup> Using Eq. (S20), a mass transfer coefficient of 1.64 m/s was calculated. The density of the bed was 4 g/mL, and the reaction order with respect to  $H_2$  was 1.07. Using such values, Mears' criterion for external mass transfer limitations was calculated to be  $1.75 \times 10^{-3}$ . This value is much smaller than 0.15, and therefore external transfer limitations can be neglected.

## V. Approach to equilibrium calculation

To ensure the kinetic measurements were performed in a differential condition, approach to equilibrium was calculated using Eq. (S21) and Eq. (S22). This specific sample calculation shows 10% CO<sub>2</sub>/40% H<sub>2</sub>/N<sub>2</sub> flow over 5% NaNO<sub>3</sub>/5% Ru/Al<sub>2</sub>O<sub>3</sub> at 260 °C.

$$K_{eq} = \exp\left(\frac{-\Delta G}{RT}\right) \quad \text{Eq. (S21)}$$

$$\eta = \frac{P_{CH_4} P_{H_2O}^2}{P_{CO_2} P_{H_2}^4} * \frac{1}{K_{eq}} \quad \text{Eq. (S22)}$$

$$\eta = \frac{\left(\frac{0.83 \text{ kPa}}{101.3 \text{ kPa}}\right) \left(\frac{1.8 \text{ kPa}}{101.3 \text{ kPa}}\right)^2}{\left(\frac{9.0 \text{ kPa}}{101.3 \text{ kPa}}\right) \left(\frac{35.4 \text{ kPa}}{101.3 \text{ kPa}}\right)^4} * \frac{1}{6.380 * 10^6} = 3.02 * 10^{-10} \quad \text{Eq. (S23)}$$

Using -69.4 kJ/mol for  $\Delta G_{533K}$ ,  $K_{eq}$  of  $6.380 * 10^6$  can be obtained from Eq. (S21).<sup>8</sup> Using the equilibrium constant obtained and partial pressures of different components of CO<sub>2</sub> methanation reaction, obtained from experiment in the given condition,  $\eta = 3.02 * 10^{-10}$  is obtained, as shown in Eq. (S23). The obtained value is orders of magnitude smaller than 1, indicating that the reaction is operating under differential conditions.

## References

- (1) Park, S. J.; Kim, Y.; Jones, C. W. NaNO<sub>3</sub>-Promoted Mesoporous MgO for High-Capacity CO<sub>2</sub> Capture from Simulated Flue Gas with Isothermal Regeneration. *ChemSusChem* **2020**, *13* (11), 2988–2995.
- (2) Karelovic, A.; Ruiz, P. Mechanistic Study of Low Temperature CO<sub>2</sub> Methanation over Rh/TiO<sub>2</sub> Catalysts. *J. Catal.* **2013**, *301*, 141–153.
- (3) Thermophysical Properties of Fluid Systems. National Institute of Standards and Technology, U.S. Department of Commerce, <https://webbook.nist.gov/chemistry/fluid/>
- (4) P.B. Weisz, C.D. Prater, Interpretation of Measurements in Experimental Catalysis, *Adv. Catal.* **6** (1954) 143–196. [https://doi.org/10.1016/S0360-0564\(08\)60390-9](https://doi.org/10.1016/S0360-0564(08)60390-9)
- (5) S. Mondal, H. Malviya, P. Biswas, Kinetic Modelling for the Hydrogenolysis of Bio-glycerol in the Presence of a Highly Selective Cu–Ni–Al<sub>2</sub>O<sub>3</sub> Catalyst in a Slurry Reactor, *React. Chem. Eng.* (2019) 595–609. <https://doi.org/10.1039/c8re00138c>.
- (6) M. Mohagheghi, G. Bakeri, M. Saeedizad, Study of the Effects of External and Internal Diffusion on the Propane Dehydrogenation Reaction over Pt-Sn/Al<sub>2</sub>O<sub>3</sub> Catalyst, *Chem. Eng. Technol.* **30** (2007) 1721–1725. <https://doi.org/10.1002/ceat.200700157>.
- (7) D.S. Scott, K.E. Cox, Temperature Dependence of the Binary Diffusion Coefficient of Gases, *Can. J. Chem. Eng.* **38** (1960) 201 <https://doi.org/10.1002/cjce.5450380605>
- (8) D.R. Stull, E.F. Westrum Jr., G.C. Sinke, *The Chemical Thermodynamics of Organic Compounds*, Wiley, 1969.

